Combined Beamforming and Scheduling for High Speed Downlink Packet Access

Alexander Seeger

Information and Communication Mobile
Siemens A.G.
Hofmannstr.51, 81359 Munich, Germany
Alexander.Seeger@siemens.com

Marcin Sikora[†]

Department of Electrical Engineering
University of Notre Dame
Notre Dame, IN 46556, USA
msikora@ieee.org

Wolfgang Utschick

Inst. for Circuit Theory and Signal Proc.
Munich University of Technology
80290 Munich, Germany
utschick@nws.ei.tum.de

Abstract—**Joint operation of High Speed Downlink Packet Access (HSDPA) and adaptive antennas in a WCDMA cellular network is considered. The total throughput per cell of HSDPA depends heavily on the strategy employed by the scheduler. It is argued that the *maximum SIR* scheduler, which maximizes throughput in the single antenna system by serving only the user with best momentary channel quality, will not substantially benefit from adaptive antennas due to excess self interference at the receiver. As an alternative a set of scheduling strategies is proposed, which rely on serving simultaneously multiple spatially separated users. System level simulations show that with the Spatial Division Multiple Access scheduler it is possible to achieve almost twofold throughput improvement over *maximum SIR* when using four antennas per sector.**

I. INTRODUCTION TO HSDPA IN CONJUNCTION WITH DOWNLINK BEAMFORMING

Rapid variations in the quality of a radio channel (fading) pose a problem for the digital transmission of voice in a cellular network, due to the strict requirements on data rate and transmission delay. One of the techniques to deal with changing channel, used e.g. in UMTS, is fast power control. The same approach can also be used for the transmission of packet data; however, relaxed requirements on rate and delay of the latter make different link adaptation techniques much more efficient. HSDPA, a part of UMTS standard responsible for downlink transmission of packet data, facilitates Adaptive Modulation and Coding (AMC), Hybrid Automatic Repeat Request (H-ARQ) and transmission scheduling to achieve high data rates up to 10.8 Mbit/s per cell.

The scheduler, a base station entity responsible for dynamical assignment of radio resources to mobile stations awaiting data, uses its knowledge about the momentary channel quality to decide how many spreading codes will be assigned to each active user. The *maximum SIR* strategy, i.e., assigning in each transmission time interval (TTI) all HSDPA spreading codes to the user with best momentary channel condition, guarantees highest throughput per cell in a single antenna system. An equivalent strategy can be defined for systems with multiple antennas: in each TTI, the user with the best channel quality is determined, and served exclusively with the weight vector that maximizes the beamforming gain. However, this strategy has a considerable drawback. Since the base station directs almost the whole transmit power to a single user, the beamforming increases both received signal power

and self interference. Effectively, this strategy does not significantly help users with good channel qualities, which generally experience much higher intracell interference than intercell interference. Since these users are most often selected by the maximum SIR scheduler, the performance increase due to application of adaptive antennas is expected to be small.

An additional disadvantage of maximum SIR scheduler used in conjunction with closely spaced adaptive antennas (i.e., a grid of beams) is the generation of rapidly changing spatial interference patterns. Such effect is caused by the fact, that in each TTI most of the base station power will be radiated in a different direction. This will cause huge time variations of both intra- and intercell interference, which can seriously impact channel quality estimation at the mobile stations. It is interesting to note that the problem of increased intracell interference is not present, when adaptive antennas are used to simultaneously serve multiple users with different weight vectors and fractions of the total base station power. However, serving multiple users simultaneously reduces the selection gain [5],[6].

Within this paper, scheduling strategies offering a compromise between both objectives are proposed. The content is structured as follows. System and propagation models are discussed in Section 2. Section 3 describes the concept of joint scheduling and beamforming and proposes two scheduler algorithms, with their performance evaluated in Section 4 based on simulation results. Finally, Section 5 draws the conclusions.

II. SYSTEM MODEL

A. Propagation model

The large-scale model of a cellular system considered in this paper assumes a hexagonal grid of cells with uniform user distribution and base stations with three sectors per site. To avoid boundary effects, two rings of adjacent base stations are simulated but only the data from the central cell is evaluated. Sectorization is achieved by directional antennas. The average channel attenuation from each BS to each MS follows exponential path loss and lognormal shadowing. Based on the average received power (proportional to the directional antenna gain and inversely proportional to the channel attenuation) each MS performs a cell selection emulating a standard handover process.

Each sector is served with a uniform linear array of N_{ant} closely spaced antennas. The channel between the BS and MS is subject to frequency selective fading, modeled in baseband as tap delay line with N_{tap} temporal taps with coefficients following zero-mean complex Gaussian distribution. Every channel coefficient vector $\mathbf{h}_m$ from all BS antenna elements for the m-th temporal tap is spatially correlated and $\mathbf{R}_\mathbf{h}[m] = E[\mathbf{h}_m \mathbf{h}_m^H]$ equals

$$\mathbf{R}_\mathbf{h}[m] = L_{avg} \cdot L_m \cdot \int_{-\pi}^{\pi} \mathbf{a}(\phi - \phi_0) \mathbf{a}^H(\phi - \phi_0) f_\Phi(\phi) d\phi , \quad (1)$$

where L_{avg} is the average path attenuation (due to path loss and shadowing), L_m is the relative power of the m-th tap and $\mathbf{a}(\phi)$, ϕ_0 and $f_\Phi(\phi)$ are the antenna array steering vector, direction of departure and the power azimuth spectrum, respectively.

An important simplification is the assumption of interference-limited system. Such assumption can be made for urban scenarios, where the cells are small, base stations are placed densely, and intercell interference always dominates over thermal noise at the mobile station receivers.

B. Transmission with multiple antennas

There are three approaches using multiple antennas at the BS for downlink communication standardized in WCDMA: uplink-based beamforming (grid of beams), closed-loop transmit diversity and open-loop transmit diversity (space-time coding). It is interesting to note that diversity techniques do not offer a considerable benefit for HSDPA, since their purpose is reduction of channel quality variations due to fading, which is the source of scheduling gain. Thus only the grid of beams approach is considered here.

The transmitter employs CDMA to send a superposition of M parallel data streams. Baseband signal $s_{(d)}(t)$ conveying d-th data stream, carries $\beta_{(d)}$ fraction of total transmit power P_T, and uses spreading factor $SF_{(d)}$ and antenna weight vector $\mathbf{w}_{(d)}$. The total transmitted baseband signal is

$$\mathbf{x}(t) = \sqrt{P_T} \sum_{d=1}^{M} \mathbf{w}_{(d)} \sqrt{\beta_{(d)}} s_{(d)}(t). \quad (2)$$

The intercell interference, just as the usable signal, is affected by path loss, shadowing, antenna gain and fading to each of the interfering sites. In such case, the radiation pattern of k-th interfering base station sector can be described by a transmission covariance matrix $\mathbf{R}_\mathbf{x}^{(k)}$,

$$\mathbf{R}_\mathbf{x}^{(k)} = E[\mathbf{x}^{(k)}(t) \mathbf{x}^{(k)}(t)^H], \quad (3)$$

where $\mathbf{x}^{(k)}(t)$ is the signal transmitted from all antenna elements of Node-B and sector k. The overall received intercell interference power can be calculated as a sum of received power from all non-serving Node-B sectors:

$$I_{inter} = \sum_{k=1}^{N_{sectors}} \sum_{i=1}^{N_{taps}^{(k)}} \mathbf{h}_i^{(k)H} \mathbf{R}_\mathbf{x}^{(k)} \mathbf{h}_i^{(k)} . \quad (4)$$

C. RAKE receiver and SIR calculation

Each mobile station is assumed to use an idealized RAKE receiver with perfect channel knowledge, one RAKE finger per channel temporal tap, and ideal maximum ratio combining (MRC). With these assumptions it is possible to calculate the SIR in the de-spread complex data sequence leaving MRC unit. The complex coefficient between the d-th data stream and i-th RAKE finger can be calculated as

$$f_i^{(d)} = \mathbf{w}_{(d)}^H \mathbf{h}_i \sqrt{P_T \beta_{(d)}} . \quad (5)$$

If the j-th RAKE finger is using the spreading code of the data signal δ, then all data signals received at other temporal tap than j are source of intracell interference,

$$SIR_j^{(\delta)} = \frac{SF_{(\delta)} \cdot \left| f_j^{(\delta)} \right|^2}{\sum_{\substack{i=1 \\ i \neq j}}^{N_{taps}} \sum_{d=1}^{N_d} \left| f_i^{(d)} \right|^2 + I_{inter}} . \quad (6)$$

After maximum ratio combining the overall SIR is

$$SIR_{MRC}^{(\delta)} = \sum_{j=1}^{N_{taps}} SIR_j^{(\delta)} , \quad (7)$$

which can be used to approximate the WCDMA modulator, beamformer, channel and RAKE receiver as an equivalent AWGN channel (on a TTI-wise basis).

D. Link-level performance of HSDPA

The dependency between SIR and throughput has been established by link-level simulations in [2]. For the assumed subset of allowed modulation and coding schemes (QPSK with rates ¼, ½, ¾ and 16-QAM with rates ½, ¾), the link level performance is shown in Fig. 1. From these throughput curves, the convex hull is taken to determine the achieved data rate as a function of signal-to-interference ratio. Note that these link level results already include possible retransmissions. The SIR value is assumed to be constant for subsequent hybrid ARQ retransmissions.

III. COMBINED SCHEDULING AND BEAMFORMING

A. Spatially separating scheduler

The SIR at the receiver listening to one of the spreading codes considerably depends on the weight vectors applied to this code (influence on usable signal power), as well as vectors applied to the remaining codes (influence on intracell interference).

The following strategy, subsequently called *spatially separating* scheduler, attempts to serve several spatially separated users simultaneously in each TTI. In the grid of beams scenario, the scheduler considers two users to be spatially separated if they are served with non-overlapping beams. The number of separated users can never exceed the number of antennas. In the first step, all mobile stations are partitioned into groups with the same serving antenna weight
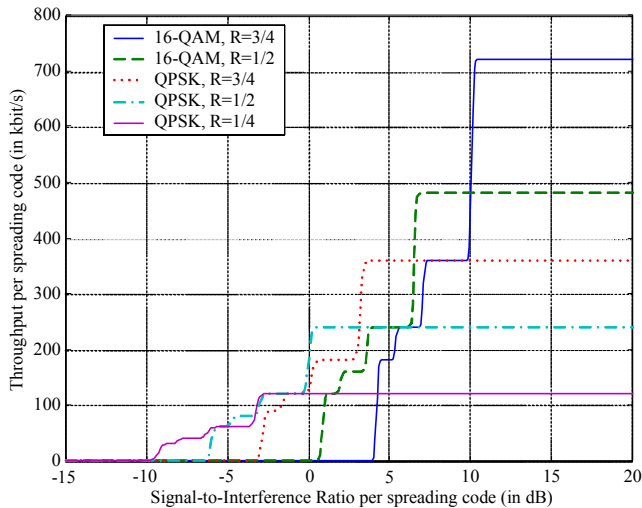
Figure 1.   Link level performance of selected modulation and coding schemes.

vector or beam. Within each group, the user with best channel quality is determined (unless the group is empty), and the remaining users are not further considered for transmission. As a next step, the scheduler constructs all possible sets of spatially separated users (sets with only one user are also considered), and tries to determine, which of them achieves the highest total throughput. After the best set is determined, the 15 HS-DSCH spreading codes are split among the users contained in this set.

Determining the best set of users is complicated by the fact, that the scheduler does not exactly know how the assignment of transmit power among beams will affect the interference levels of the users. We will follow an approach in which scheduler neglects this problem and assumes that the SIR at every Rake receiver is linearly proportional to the signal power (i.e., assumes that signal power does not affect intracell interference). Thus, for each group of K users with signal-to-interference ratios $SIR_{(k)}$, $k = 1, \ldots, K$ signaled over CQI feedback, the scheduler calculates the following metric:

$$J = \sum_{k=1}^{K} \log\big(1 + SIR_{(k)}\big)/ K .$$ (8)

This metric corresponds to the sum of Shannon capacities to the selected users under the simplifying assumption mentioned above.

B.   Space Division Multiple Access scheduler

The scheduler presented in the previous section serves multiple spatially separated users simultaneously. Although the condition used to conclude spatial separation is quite simple, it promises a reduction in intracell interference especially in the grid of beams scenario. Ideally, spatial separation leads to complete elimination of such interference. In such a case, it is not necessary to use only a subset of 15 HS-DSCH spreading codes, but a full set of codes could be reused for each mobile station. Of course, in order to keep the total transmit power unchanged, the amount of power per spreading code must be

lowered. However, performing a communication on a larger bandwidth (with spreading codes corresponding to bandwidth) is more power-efficient in terms of Shannon capacity, and the code reuse can bring considerable throughput improvement. The scheduler implementing this strategy performs a *Spatial Division Multiple Access* (SDMA).

The selection process of the set of users to be served is based on the same principle as the *spatially separating* scheduler. The only difference comes in the way of calculating the metric for the set of K users:

$$J = \sum_{k=1}^{K} \log\big(1 + SIR_{(k)} / K\big).$$ (9)

Since in practice the spatial separation is not perfect, reuse of spreading codes can lead to cross-talk between two data channel using the same spreading and scrambling code. This might be undesirable, since if both channels use the same channel code, the receiver might have a problem in distinguishing both channels. This problem can be mitigated by using multiple scrambling codes in a single cell, and serving each user with different scrambling code and the full set of spreading codes. Both variants of *SDMA* scheduler (with single or multiple scrambling codes) will be considered for the grid of beams system.

IV.   SIMULATION RESULTS

The basic system simulation approach is a snapshot simulator. The complete set of simulation parameters is shown in Table 1. Performance of scheduling strategies considered for adaptive antenna systems is evaluated for two main scenarios: grid of 8 beams for 4 antennas and grid of 4 beams for 2 antennas. Fig. 2 and Fig. 3 present simulation results for the grid of beams scenario with four antennas and eight beams, at both Pedestrian A and Vehicular A delay spread profiles. The

TABLE I.   SYSTEM SIMULATION PARAMETERS.

| Parameter	Value
Number of sectors per site	3
Directional antenna pattern	see UMTS 30.03
Adaptive antenna scenarios	2 antennas, grid of 4 beams 4 antennas, grid of 8 beams
Antenna spacing	0.5 wavelength
Path loss exponent	3,76
Shadowing standard deviation	8 dB
Site-to-site shadowing correlation	50%
Sector-to-sector shadowing correlation	100%
User placement	Uniform
Serving site selection	Minimum path loss + shadowing
Power delay profile	Vehicular A, Pedestrian A
Receiver	RAKE with one finger for each tap, perfect MRC
Fraction of Node-B power dedicated to HS-DSCH	80%
Number of HS-DSCH spreading codes	15
Number of snapshots	10000
Angular spread for direction of departure	Laplace distributed with 2 deg standard deviation
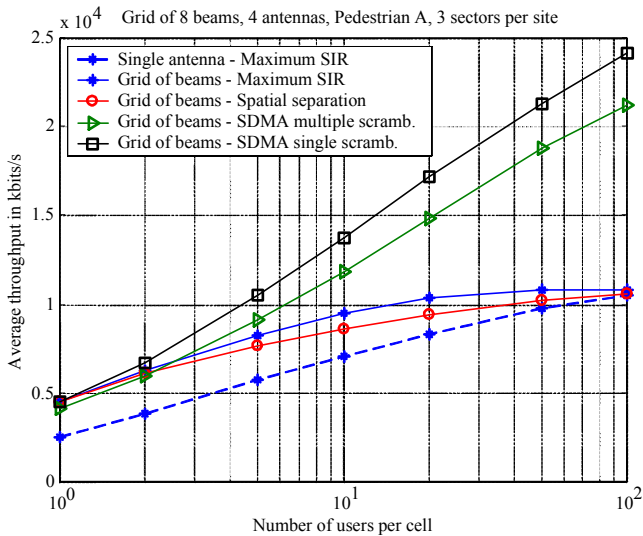
Figure 2. Average throughput per cell for different scheduler types for Pedestrian A power delay profile.
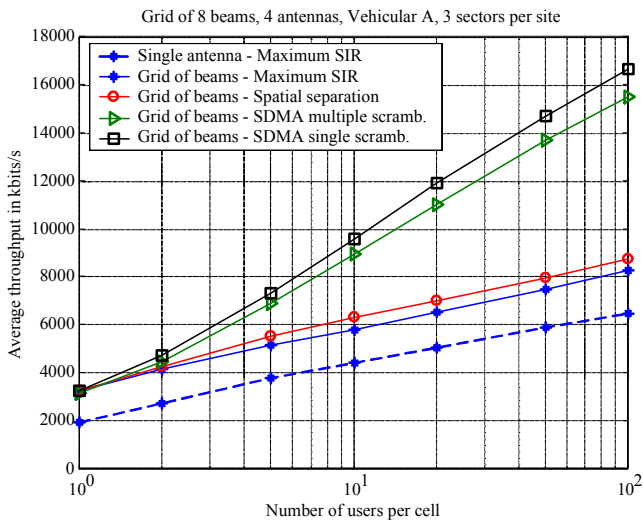

Figure 4. Distribution of SIR for Pedestrian A power delay profile.

Figure 3. Average throughput per cell for different scheduler types for Vehicular A power delay profile.
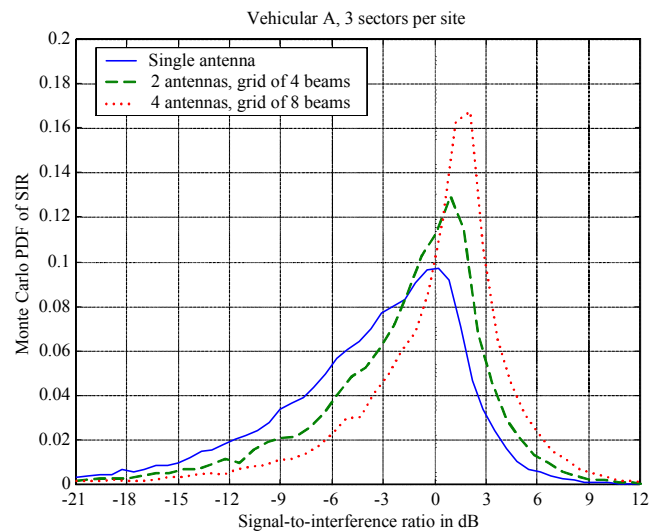
Figure 5. Distribution of SIR for Vehicular A power delay profile.

average throughput per cell for all considered schedulers is shown in comparison to a single antenna scenario with the *maximum SIR* scheduler.

For both power delay profiles, the application of 4 antennas allows the *maximum SIR* scheduler to increase the throughput by a constant offset (except for MCS saturation range), compared to single antenna case. This is due to the beamforming gain which increases the power of the usable signal by about 6 dB (4 antennas), but it also increased the intracell interference. Since intracell interference is more predominant in Vehicular A, its SIR and throughput increase is lower than in Pedestrian A.

This effect is better illustrated in the SIR distributions before scheduling for single antenna and 4 antennas as presented in Fig. 4 and Fig. 5. In upper range of SIR the distribution shifted up by 4 dB in Pedestrian A and only by 2
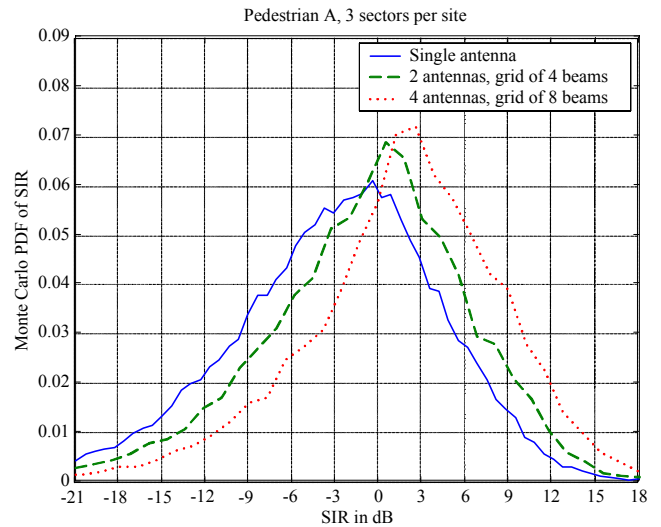
dB in Vehicular A (which is a very small benefit from having 4 antennas). In Pedestrian A, the SIR increase quickly caused throughput saturation at the maximum value allowed with highest MCS, indicating a need for even higher order modulations.

The *spatially separating* scheduler turns out to be not considerably better than *maximum SIR* scheduler. In comparison between both, *spatially separating* scheduler gains by reducing the intracell interference, but loses some of the multiuser gain. The balance of the two effects is positive for the Vehicular A, but negative for Pedestrian A.

Compared to the previous strategies, the *SDMA* scheduling offers a tremendous performance gain. Using the full set of spreading codes per user almost doubles the average throughput in Vehicular A. In Pedestrian A the gain is even higher, since the reduction of SIR (caused by splitting the same
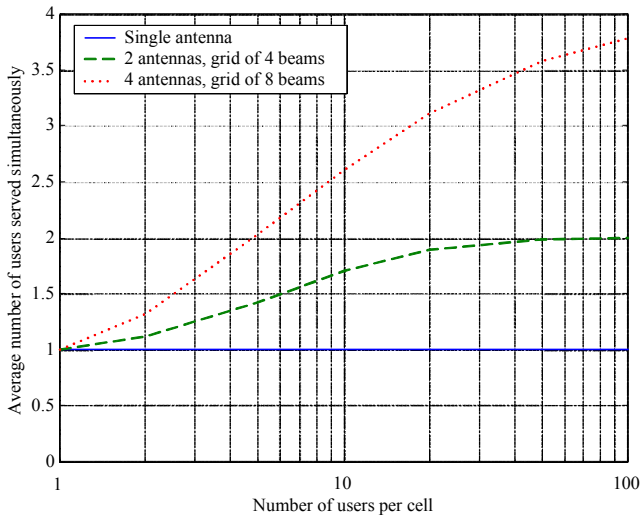
Figure 6. Number of users served simultaneously by SDMA scheduler for one, two, and four antennas, and the power delay profile "Pedestrian A".

transmission power over larger number of codes) eliminates the MCS saturation point. The throughput with *SDMA* scheduling increases much faster with the number of users than with *maximum SIR*. Responsible for this is a new type of multiuser gain, called here *spatial* multiuser gain. This gain comes from ability of *SDMA* scheduler to find larger and larger sets of mutually spatially separated users, which can be then served simultaneously. This is illustrated in Fig. 6, which shows the average number of simultaneously served users versus total number of users per cell.

Finally, Fig. 2 and Fig. 3 reveal that between two *SDMA* strategies, the variant with multiple scrambling codes was consequently worse than the one with single scrambling code. The reason for this is an excess interference coming from the common channels (using the remaining 20% of the Node-B transmit power), which are distributed evenly across all eight beams. With one scrambling code, these channels pose minimal interference to HS-DSCH, but with multiple – they interfere with HS-DSCH spreading codes located on overlapping beams using different scrambling codes.

V. CONCLUSIONS

The main conclusions from the simulation results presented are as follows.

- Using maximum SIR scheduler with adaptive antennas increases the power of the usable signal, but also increases the

intracell interference. The latter effect is particularly harmful in scenarios with wide power delay profile – in system with 4 antennas only 2 dB gain in SIR was observed. In scenarios with narrow power delay profile SIR reached high values, which could not be fully exploited due to limited range of modulation and coding schemes.

- Adaptive antennas can be used to separate users spatially. The *spatially separating* scheduler uses this ability to counteract the increase of intracell interference experienced by *maximum SIR*. It achieves this by sharing the HS-DSCH codes between multiple spatially separated users, at a cost of lower multiuser gain (selecting multiple instead of single best user). The net balance is positive only for wide power delay profile scenarios.

- The true benefit of spatial separation is enabled by the *SDMA* scheduler. By reusing all spreading codes for spatially separated users Spatial Division Multiple Access takes advantage of additional bandwidth provided by spatial dimension. As an indirect, but considerable benefit, SDMA scheduler raises the maximum throughput permitted by the highest MCS by the factor equal to number of antennas. Both effects allowed the *SDMA scheduler* to almost double the average throughput per cell, compared to *maximum SIR*. In a scenario with 4 antennas, grid of 8 beams and Pedestrian A, the average throughput reaches up to 25 Mbit/s for 50 users per cell.

REFERENCES

[1] 3GPP, TR 101 112, v3.2.0, Selection procedures for the choice of radio transmission technologies of the UMTS, 1998.

[2] M. Döttling, J. Michel, B. Raaf, "Hybrid ARQ and adaptive modulation and coding schemes for high speed downlink packet access," IEEE International Symposium on Personal, Indoor and Mobile Radio Communications, pp. 1073 -1077, 2002.

[3] K.I. Pedersen, P.E. Mogensen, B.H. Fleury, "A Stochastic Model of the Temporal and Azimuthal Dispersion Seen at the Base Station in Outdoor Propagation Environments," IEEE Trans. Vehicular Technology, vol. 49, no. 2, pp. 437-447, Mar. 2000.

[4] 3GPP, TR 25.877 Technical Report on Beamforming Enhancements.

[5] D.J. Mazzarese and W.A. Krzymień, "High throughput downlink cellular packet data access with multiple antennas and multiuser diversity," in Proc. IEEE Vehicular Technology Conference, pp. 1079-1083, April 2003.

[6] H. Viswanathan and K. Kumaran, "Rate scheduling in multiple antenna downlink wireless systems", in Proc. Allerton Conference on Communications and Control, October 2001.